

## **The Free Retraction of Natural Rubber: A momentum-based model**

Lewis B. Tunnicliffe<sup>a,b,†</sup>, Alan G. Thomas<sup>a,b</sup>, James J.C. Busfield<sup>a,b,‡</sup>

<sup>a</sup>Materials Research Institute, Queen Mary University of London, Mile End Road, London, E1 4NS, United Kingdom

<sup>b</sup>School of Engineering and Materials Science, Queen Mary University of London, Mile End Road, London, E1 4NS, United Kingdom

<sup>†</sup>Corresponding author during the submission and review process

<sup>‡</sup>Corresponding author post-publication

l.tunnicliffe@qmul.ac.uk +44 (0)7951248541

a.g.thomas@qmul.ac.uk

j.busfield@qmul.ac.uk +44 (0)20 7882 8866

## **Abstract**

The free retraction of vulcanised strips of natural rubber released from simple uniaxial deformations is studied using high speed cinematography in the context of a simple momentum theory. A good agreement between the theory and experiment is observed when vulcanisates are released from stresses below 1 MPa which corresponds to tensile strains rates below  $1 \times 10^3 \text{ s}^{-1}$ . Above this critical stress and corresponding strain rate value, an increasing dispersion is observed in the form of a slowing down of the characteristic retraction pulse and also by a relaxation of strain ahead of the pulse front (a dispersion of the pulse). Holding samples at high strains for an extended period of time prior to releasing results in a further, significant retardation of the retraction pulse velocity. These effects are related to the increasing non-linearity of high strain rate retraction stress-strain behaviour. Energy balance arguments show that the dispersion of the retraction pulse is a prerequisite for pulse propagation and its magnitude underpins the deviation from the momentum model outlined in this paper.

## **Keywords**

Rubber, free retraction, strain-induced crystallisation, viscoelasticity, high strain rate, elasticity

## 1. Introduction

Elastomeric materials are often used in applications where they must undergo very large and very rapid cyclic loadings. Obtaining reliable experimental data at such high strains and strain rates can be very challenging. As such, many issues surrounding the physics of high speed fracture and large strain dynamic processes lack detailed experimental investigation. Efforts have been made to characterise the loading [1] and fracture [2,3] properties of rubbers at very high strain rates, whereas the characterisation of rapid unloading of rubber has received less attention. A number of papers have addressed rapid unloading by examining the free retraction of rubber - where rubber is deformed and then released [4-11], or released from tension post-fracture e.g. after the bursting of a rubber balloon [12].

Mrowca, Dart and Guth [4,5] noted that when released from moderate extensions, tensile retraction of rubber strips proceeds via a retraction pulse which travels through the material at a velocity,  $v$ , relaxing the strained portion as it proceeds. A schematic of this free retraction process is given in Figure 1. James and Guth [6] proposed a simple theoretical model of tensile retraction by considering the wave equation. They assumed that the retraction pulse propagates through a Hookean material (linear shear stress-strain relation) without any dissipation from the internal viscosity of the polymer and found a reasonable agreement to their solution for the velocity of the pulse with experimental data collected for free retractions from small extensions:

$$v = (\lambda_0 + 1) \sqrt{\frac{E}{\rho}} \quad 1$$

Where  $E$  is the Young's modulus of the material,  $\lambda_0$  is the strain in the material prior to releasing and  $\rho$  is the material density.

Mason [7-9] later developed a more rigorous treatment of the process by taking into account the non-linear nature of rubber elasticity and the high strain rate stress-strain retraction curve. He showed that if the retraction process is considered in terms of infinitesimal time steps, the velocity of volume elements of material along the strip of rubber relative to the fixed (clamped) end,  $\varphi$ , depends on the instantaneous modulus,  $E_i = \partial\sigma/\partial\lambda$ , giving:

$$\frac{\partial\varphi}{\partial\lambda} = -\sqrt{\frac{E_i}{\rho}} \quad 2$$

This relation allows for the experimental determination of retraction stress-strain data by accurate measurement of  $\varphi(\lambda)$ . Mason showed that dispersion of the retraction pulse - that is a spreading out of the retraction pulse along the rubber strip - which is observed experimentally in rubbers released from sufficiently high extensions, arises from the non-linearity of rubber elasticity at large extensions. Thus, upon release, the head of the retraction pulse proceeds rapidly through highly extended material of very high  $E_i$  while the trailing end of the pulse proceeds less rapidly through partially unloaded material of lower  $E_i$ .

Gent and Marteny [10] again demonstrated that both the velocity of retraction pulses and the velocity of sound waves propagated through strained rubber are dictated by the instantaneous modulus of elasticity.

Bogoslovov and Roland [11] applied Mason's approach to compute stress-strain relationships for the high strain rate retraction of polybutadiene and polyurea rubbers. They pointed out that the obtained stress-strain curves are somewhat complicated by the transient strain rates experienced by individual volume elements of the material during retraction.

Stevenson and Thomas [12] studied free retraction in the context of the bursting of rubber balloons. Here rubber retracts from an imposed biaxial strain following a point fracture of the material. They derived a theoretical analysis, distinct from Mason's approach, in terms of momentum concepts and found a reasonably good agreement between their theory and experimental values for the observed retraction velocity,  $u$ , (in their images the retraction pulse was too small to be observable so no values of  $v$  were reported).

This paper modifies the momentum theory proposed by Stevenson and Thomas for the case of uniaxial free retraction and examines its applicability to the free retraction of natural rubber (NR) strips released from finite tensile extensions.

## 2. Theory

The unstrained width and thickness of the sample strip are  $w$  and  $h$  respectively, giving the strained cross-section as  $wh / \lambda$ . As retraction proceeds, more material is relaxed to the unstrained state, which is moving at velocity  $u$ . The rate of increase of mass of material, having density  $\rho$ , in the unstrained region is given by:

$$\frac{\Delta(vol)\rho}{\Delta t} = \frac{vwh\rho}{\lambda} \quad 3$$

and thus the rate of increase in momentum is  $vwh\rho u/\lambda$ . This is equal to the force  $\alpha wh/\lambda$  and so the stress is given by:

$$t = vu\rho \quad 4$$

Due to the incompressibility of rubber, the total volume of the material remains constant during retraction which gives:

$$wh(v - u) = \frac{vwh}{\lambda} \quad 5$$

Solving Equations 2 and 3 for  $u$  and  $v$  gives:

$$v = \sqrt{\frac{t\lambda}{\rho(\lambda - 1)}} \quad 6$$

$$u = \sqrt{\frac{t}{\rho} \left( \frac{\lambda - 1}{\lambda} \right)} \quad 7$$

and

$$\frac{v}{u} = \frac{\lambda}{(\lambda - 1)} \quad 8$$

Note that  $t$  is the true stress, and the measured force is usually expressed as the nominal stress,  $\sigma$ , referred to the unstrained cross-section given by  $\sigma = t/\lambda$ , therefore:

$$v = \sqrt{\frac{\sigma\lambda^2}{\rho(\lambda - 1)}} \quad 9$$

$$u = \sqrt{\frac{\sigma(\lambda - 1)}{\rho}} \quad 10$$

## Experimental

### 2.1. Sample Preparation

Samples were prepared using a Carter 2-roll laboratory mill. The rubber used was SMR-CV60 grade Natural Rubber (NR). The NR was compounded with a cure package detailed in Table I. The total loading of sulphur was varied in order to produce samples with a chosen range of crosslink densities. However the sulphur to accelerator loading ratio was maintained at 1:1 to ensure comparability of the chemical nature of crosslinks between compounds in terms of the number of sulphur atoms which constitute a chain-chain link. A black-coloured anti oxidant chemical (6PPD) was included in the cure package to produce darker coloured vulcanisates with a matt surface finish in order to improve video image contrast and reduce reflection from the sample surface. Cure characteristics of these compounds were measured on an Alpha Technologies MDR2000 rheometer with platen temperatures of 160 °C. Rectangular strip samples of approximately 25x1.5x60 mm were prepared by compression moulding sheets of rubber on a laboratory hotpress at a plate temperature of 160°C. The cure time corresponding to the maximum in the torque-time trace was determined using a MDR2000. Subsequently, strips of samples having a width of 6 mm and a thickness of 1.5 mm were stamped from the sheets using a pneumatic die cutter.

### 2.2. Equilibrium Solvent Swelling Measurements

Equilibrium solvent swelling experiments were performed in a fumehood using toluene solvent. Samples of crosslinked rubber (~0.2 g) were immersed in 100 ml of toluene and then removed every 24 hours and weighed on a 4-point balance after ensuring that excess solvent at the sample surface was removed by lightly dabbing the surface with tissue. This process was repeated for 84 hours and during this period the samples were stored in the dark to avoid photo-oxidative breakdown of the crosslinked networks [13]. Three repeats were performed per sample. For this paper, in order to define the crosslink density we use the affine description of network elasticity, take the polymer-solvent interaction parameter for NR-toluene as 0.393 and NR density as 0.92 g.cm<sup>-3</sup>. Values of crosslink density were calculated in units of mol.g<sup>-1</sup> using the well known Florey-Rehner equation [14]. Values are reported in Table I.

### 2.3. Quasi-static cyclic tensile Measurements

Quasi-static cyclic tensile measurements were performed for each compound using an Instron 5566 test frame with a 1 kN capacity load cell and a video strain gauge. Samples were extended to an initial extension ratio of  $\lambda = 2$  then retracted to a load condition of 0 N. This process was then

repeated with increasing extension ratios of 3, 4 and 5. The strain rate of the deformation was 0.03 /s.

#### 2.4. Free Retraction Measurements

Free retraction measurements were performed at room temperature using an Instron 5566 screw driven tensiometer to provide the sample deformation and record the resulting force using 1 kN load cell. Sample strips were clamped top and bottom into the Instron frame. The top clamp was attached directly to the load cell and so was permanently clamped onto the sample for the duration of the test. The lower clamp was actuated via a motorised, geared screw thread system allowing it to be opened very rapidly and thus cleanly releasing the sample. Due to the natural tack of the rubber compounds, at low extensions ratios some of the samples were found to adhere for a few milliseconds to the bottom clamp after being released. To circumvent this problem a small amount of sellotape was applied to the lower section of the sample strip in the clamping region in order to lubricate the release of the sample.

A Vision Research Phantom V7.3 (monochrome) high speed video camera was used to collect video images of the free retraction process. The high speed camera was set up parallel to the mounted strips of rubber. The system was calibrated with the sample in the un-deformed state by taking a still picture of the setup with a ruler in the frame to provide scale. For a typical calibration 1 pixel = 0.4 mm. The high speed camera was set to collect 38,000 images per second and could be remotely triggered just prior to the free retraction process. In order to collect sufficiently exposed images, two Lilliput 150ce spotlight lamps were positioned at either side of the high speed camera in order to illuminate the sample. The lamps had a combined power output of 1300 W meaning that warming of the samples and load cell could lead to unwanted artefacts in the data. To avoid this, the lamps were operated only for the 2-5 seconds of the duration of testing. A reflective heat shield was also placed over the load cell. In order to precisely determine sample displacements, a series of horizontal fiducial markers were drawn on to the tensile strips 5 mm apart. The procedure for the free retraction measurements was as follows: a target extension ratio ( $\lambda$ ) was imposed on the rubber samples ( $\lambda = 2, 3, 4$  or  $5$ ) at a crosshead displacement rate of 100 mm/minute ( $\dot{\epsilon} \sim 0.03$  /s) and the resulting tensile forces were recorded. As soon as the desired strain level was achieved, the camera lamps were switched on, the camera was remotely activated and the bottom clamp was released. The high speed camera recorded digital video footage for total of 6 seconds following the trigger (the total retraction time of the strips was of the order of several milliseconds). A fresh sample was used for each strain level measurement. Samples tested in this way are termed 'instantaneously-released' samples.

A second series of experiments was performed whereby a sample of each compound was deformed to a target extension ratio of 5 and held for 1 hour in the deformed state to promote the formation of strain-induced crystallites prior to free retraction measurement. The associated relaxation of tensile force during this period was also recorded. Samples tested in this way are termed 'delayed release' (DR) samples. Holding samples at such high strains promotes the growth of strain induced crystallites. For example Toki and co-workers [15] reported for similar materials held under similar mechanical conditions, a crystalline content of around 15 % at  $\lambda = 5$ .

The resulting video images were subsequently digitally analysed (Phantom high speed camera software) and experimental values for  $v$  and  $u$  as well as the maximum strain rates were calculated. Values of  $\sigma$ , defined in the introduction as the nominal stress, were calculated from the value of force recorded just prior to releasing of the samples normalised to the un-deformed cross sectional area of the samples. Precise values of  $\lambda$  were determined from digital image analysis (note that the applied strain was simply a target strain and the actual extension ratios of the samples varied slightly from the imposed strain calculated from the crosshead displacement).

### 3. Results and Discussion

Figure 2 shows cyclic stress-strain behaviour for the three vulcanised compounds collected at room temperature using a low rate of tensile strain ( $\dot{\epsilon} = 0.03$  /s). The increase in cyclic hysteresis with increasing maximum extension is marked. When the materials are cycled up to a peak extension ratios of  $\lambda = 3$  the materials are highly elastic, displaying little hysteresis. At peak extension ratios of  $\lambda = 4$  and  $\lambda = 5$ , there is significantly more dissipation of energy (hysteresis). This is related to the formation and melting of strain-induced NR crystallites and crosslink or polymer chain rupture. In Figure 3 the incremental moduli observed upon initial retraction of the materials from the maximum extension of  $\lambda = 5$  at a strain rate of 0.03 /s is shown.

Figures 3 & 4 show the correlation between the experimental and theoretical values of  $u$  and  $v$ . The solid line in both plots corresponds to a  $y = x$  relationship. As can be seen in Figure 3, experimental values of  $u$  (the retraction velocity of the bottom of the rubber strip) are in excellent agreement with the theory - particularly at lower velocities  $< 60$  m.s<sup>-1</sup>. At higher velocities corresponding to higher strains and the more densely crosslinked compounds, there is some evidence of a reduction in experimental velocity versus the theory. The delayed release samples appear to be systematically slower than predicted from theory. Figure 4 plots the data for values of  $v$  (the velocity of the retraction pulse). Again, at lower velocities there is an excellent correlation between experiment and



theory. Data at higher velocities and the data for the delayed release samples show a significant divergence from the theory.

From Figures 4 & 5, it appears as if the lower velocity retraction processes are in agreement with the momentum-based theory outlined in Section 2. However a significant deviation from the theory becomes apparent at release stresses (and corresponding maximum strain rates) above a critical value. This value was determined by plotting the deviation from theory of the experimentally-determined velocities for the retraction pulses of the two highest extension ratios against their respective release stresses (Figure 5). Despite the experimental scatter there is a clear increase in deviation from theory which is extrapolated back to an onset stress of roughly 1 MPa ( $\sim 1.1 \times 10^3 \text{ s}^{-1}$ ). The delayed release sample data is also plotted on the same graph and lie systematically above the relationship determined for the immediately released samples.

Although the theory outlined in the previous section is derived solely in terms of momentum principals, it is of interest to consider the energy change during the retraction process. The rate of increase in volume of the unstrained region is  $vwh/\lambda$ . Therefore the rate of increase in kinetic energy is  $E_R vwh/\lambda$  where  $E_R$  is the energy per unit volume released upon retraction to the unstressed state. Thus the net rate of energy loss is

$$\frac{\partial E}{\partial t} = vwh[(E_R - \frac{1}{2}\rho u^2)/\lambda] \quad 11$$

which, given Equation 10, becomes:

$$\frac{\partial E}{\partial t} = vwh[E_R - \frac{1}{2}\sigma(\lambda - 1)] \quad 12$$

Physically it would be impossible for Equation 12 to be negative (which would imply a gain in total energy), and it would be zero for a perfectly elastic material. Thus the retraction curve, taken at the appropriate (high) rate, would have to be concave towards the strain axis, which seems unlikely and is not observed in the high strain rate retraction curve data presented by Bogoslovov and Roland [11]. The conclusion would appear to be that the pulse cannot propagate without dispersion, in contradiction with the initial assumptions of the momentum theory outlined in this paper. The fact that nevertheless the theory gives quite good agreement with experiment - certainly at smaller release stresses - suggests that the departure from the assumption cannot be great.

### 3.1.1. Pulse dispersion effects

On close inspection of the video footage it is apparent that for some of the materials released from high stresses and the delayed release (more crystalline) materials, there is a significant retraction of material in advance of the main retraction pulse. Figure 6 plots the positions of the fiducial marks on the sample strip relative to the fixed end as a function of strip retraction time. For materials released from small strains, the material ahead of the retraction pulse remains in the strained position until it is relaxed by the pulse. However for materials released from higher extensions, significant relaxation of the material ahead of the pulse is observed. This is due to the increasing non-linearity of the high strain rate stress-strain retraction curve associated with finite network extensibility and the presence of strain-induced crystallites at larger strains.

## Conclusions

The free retraction of natural rubber strips released from simple extension at room temperature was examined in the context of a momentum-based model derived from previously published work. A good agreement with the theory was observed for samples released at lower stresses and corresponding strain rates. However, an increasing divergence from the theory in the form of a slowing down of the retraction pulse was apparent when release stresses were raised above  $\sim 1$  MPa. Additionally, the length of the retraction pulse was observed to increase with an increasing divergence from the theory. These effects are related to the increasing non-linearity of high strain rate retraction stress-strain behaviour. From a consideration of the energetics of the process it appears that dispersion of the retraction pulse is a prerequisite for pulse propagation and its magnitude underpins the deviation from the momentum model outlined in this paper. Follow-up work shall extend the study of the process herein described through finite element simulations.

## Acknowledgements

LBT thanks the Soft Matter Group for postdoctoral funding. The authors are very grateful for the use of the Vision Research Phantom V7.3 high speed camera which was borrowed from the EPSRC (Engineering and Physical Sciences Research Council) Engineering Instrument Pool, UK.

## References

1. L. Bateman. The chemistry and physics of rubber-like substances. 1st Ed. Maclaren & Sons, 1963
2. K. Sakulkaew, A.G. Thomas, J.J.C. Busfield. The effect of the rate of strain on tearing in rubber, *Polym Test.*, 2011;30(2):163
3. K. Sakulkaew, A.G. Thomas, J.J.C. Busfield, The effect of temperature on the tearing of rubber, *Polym Test*, 2013;32(1):86
4. B.A. Mrowca, C.S.C. Dart, E. Guth, Retraction of stressed rubber, *Phys Rev*, 1944;66(1-2):30
5. B.A. Mrowca, C.S.C. Dart, E. Guth, Photographic study of the retraction of stressed rubber, *Phys Rev*, 1944;66:(1-2)32
6. H.M. James, E. Guth, Theory of the retraction of stressed rubber, *Phys Rev*, 1944;66(1-2):32
7. P. Mason, Propagation of finite elastic waves in rubber, *Nature*, 1959;183():812
8. P. Mason, Longitudonal wave propagation in stretched polymers, *J Appl Phys*, 1960;31:1706
9. P. Mason, Finite elastic wave propagation in rubber, *Proc. Royal Soc. A*, 1963;272:315
10. A.N. Gent, P. Marteny, The effect of strain upon the velocity of sound and the velocity of free retraction for natural rubber, *J Appl Phys*, 1982;53:6069
11. R.B. Bogoslovov, C.M. Roland, Viscoelastic effects on the free retraction of rubber, *J Appl Phys*, 2007;102:063351
12. A. Stevenson, A.G. Thomas, On the bursting of a balloon, *J Phys D Appl Phys*, 1979;12:2101
13. J.L. Valentín, J. Carretero-González, I. Mora-Barrantes, W. Chassé, K. Saalwächter, Uncertainties in the determination of cross-link density by equilibrium swelling experiments in natural rubber, *Macromolecules*, 2008;41:4717

14. L.R.G Treloar. The physics of rubber elasticity. 3rd ed. Oxford University Press, 2009

15. S. Toki, I. Sics, B. S. Hsiao, M. Tosaka, S. Poompradub, Y. Ikeda, S. Kohjiya, New insights into structural development in natural rubber during uniaxial deformation by in situ synchrotron X-ray diffraction, *Macromolecules*, 2002;38:7064

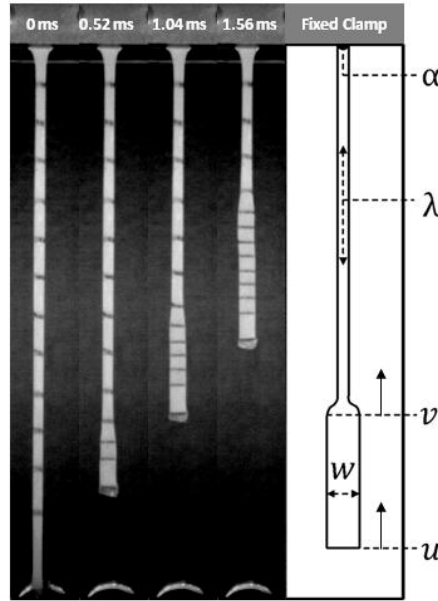


Figure 1: The free retraction of a strip of rubber. Left: experimental image. Right: Schematic overview of the process where  $u$  is the velocity of the bottom of the strip,  $w$  is the width of the relaxed section of the strip,  $v$  is the velocity of the retraction pulse travelling through the strip,  $\lambda$  is the extension ratio and  $t$  is the true stress measured at the fixed clamp. The direction of retraction is from bottom to top

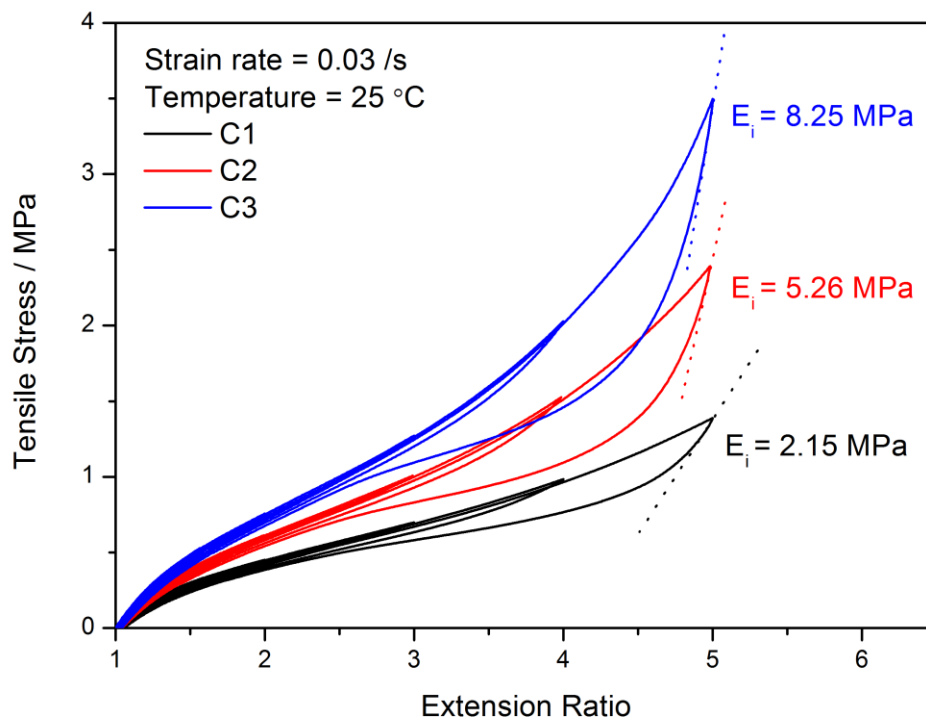


Figure 2: Cyclic stress-strain data for each compound used in the study (C1, C2, C3). Compounds were cycled to  $\lambda = 2,3,4$  and 5. The instantaneous moduli measured upon initial retraction from  $\lambda = 5$  are indicated

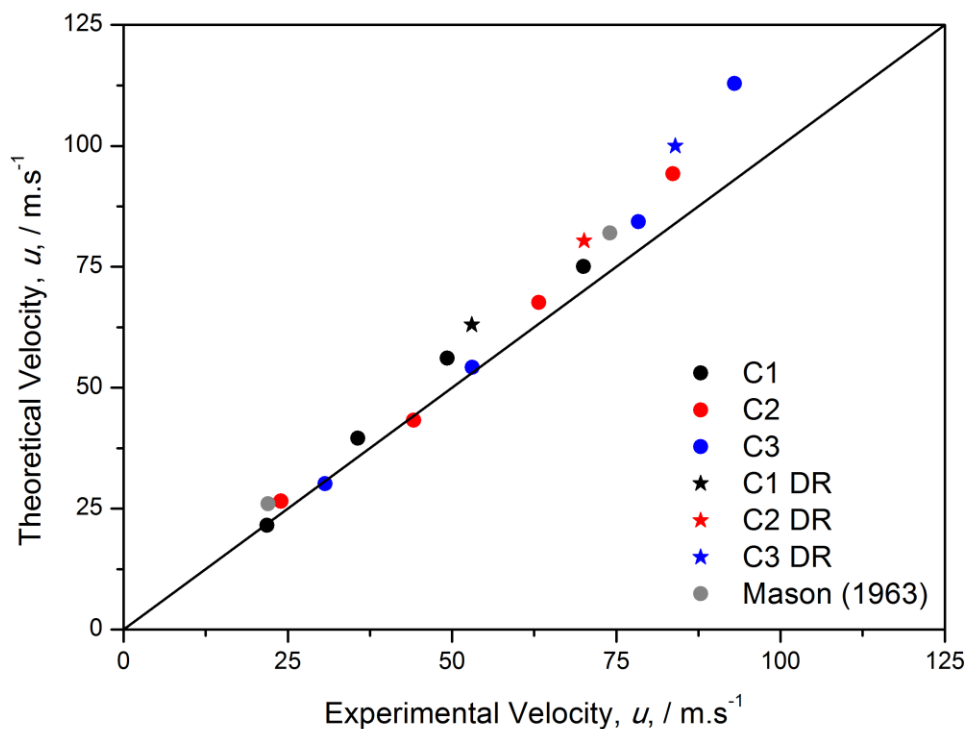


Figure 3: Correlation of the experimentally-determined value of the velocity of the bottom of the rubber strip undergoing a free retraction,  $u$ , with values calculated from the theory based on momentum considerations as outlined in the introduction. The solid corresponds to  $y = x$ . The literature values of Mason [9] are included for comparison. C1, C2 and C3 refer to 'instantaneous-release' data from compounds 1-3 respectively. C1 DR, C2 DR and C3 DR refer to 'delayed release' data from compounds 1-3 respectively

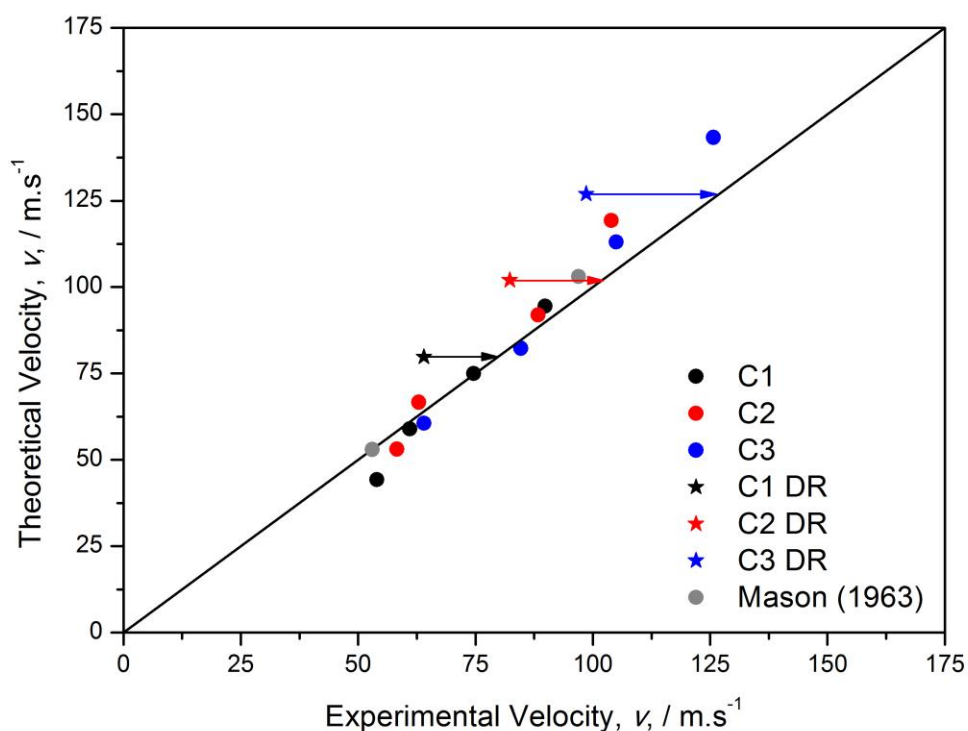


Figure 4: Correlation of the experimentally-determined value of the velocity of the retraction pulse,  $v$ , with values calculated from the theory based on momentum considerations as outlined in the introduction. The solid corresponds to  $y = x$ . Literature values from Mason [9] are included for comparison. C1, C2 and C3 refer to 'instantaneous-release' data from compounds 1-3 respectively. C1 DR, C2 DR and C3 DR refer to 'delayed release data from compounds 1-3 respectively. Coloured arrows illustrate the systematic deviation from theory shown by the 'delayed release' (DR) samples

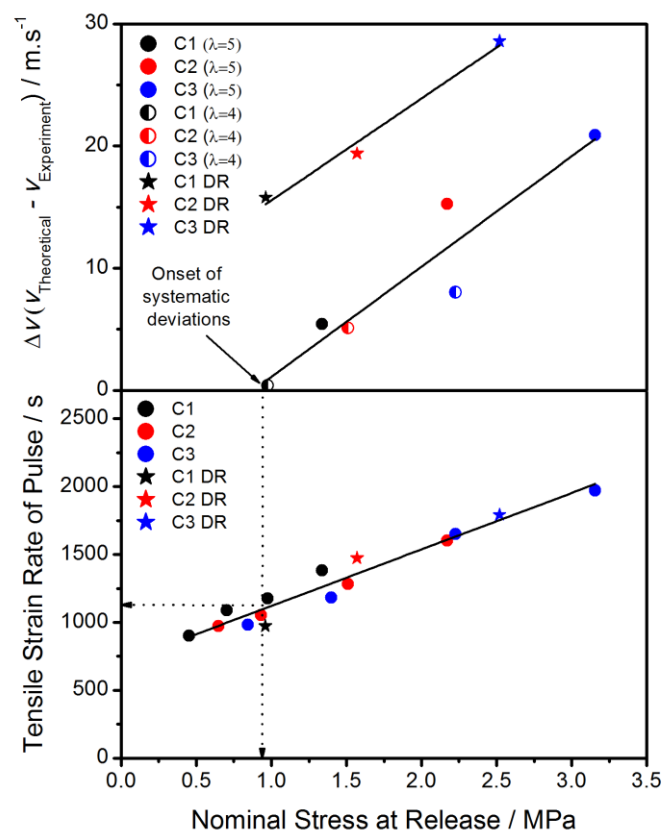


Figure 5: (Top) Difference in retraction pulse velocity between theory and experiment plotted as a function of the stress at release. (Bottom) Tensile strain rates of the retraction pulse calculated from the velocity of the retraction pulse normalised to the initial sample length. The stress and strain rate at which significant deviations from the theory are observed are indicated with dotted lines. C1, C2 and C3 refer to 'instantaneous-release' data from compounds 1-3 respectively. C1 DR, C2 DR and C3 DR refer to 'delayed release data from compounds 1-3 respectively



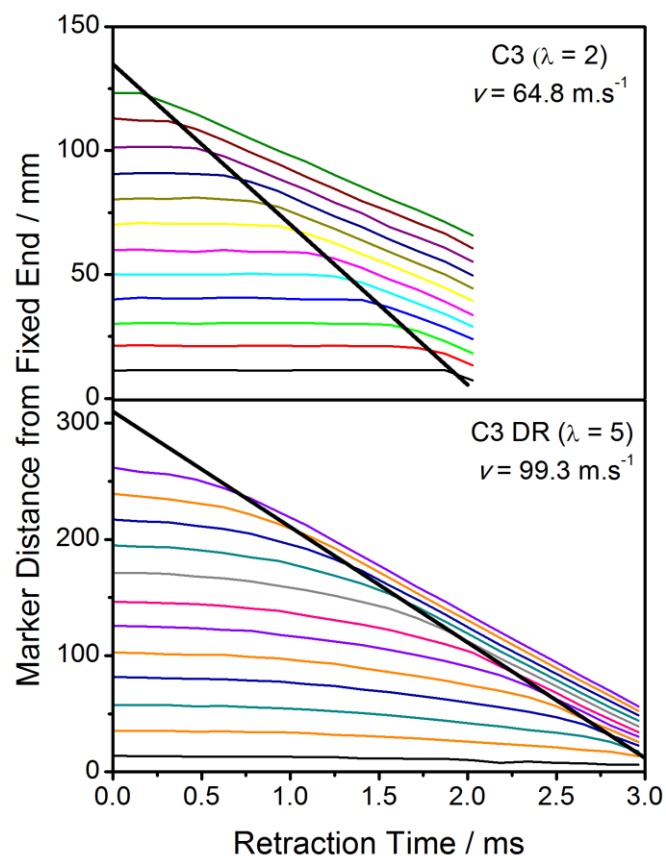


Figure 6: Position of the fiducial marks on the retraction samples relative to the fixed end as a function of the free retraction time for C3 released from  $\lambda = 2$  (top) and  $\lambda = 5$  with delayed release (bottom). The velocity of the tip of the retraction pulse is indicated by the solid black lines. Note the difference in y axis scale between samples.

Curative /phr <sup>A</sup>	Compound 1 (C1)	Compound 2 (C2)	Compound 3 (C3)
Sulphur	1	1.5	2
CBS <sup>B</sup>	1	1.5	2
Zinc Oxide	5	5	5
Stearic Acid	2	2	2
6PPD <sup>C</sup>	3	3	3
Crosslink Density, $\times 10^5$ / mol.g <sup>-1</sup>	5.14	7.86	9.39

<sup>A</sup>phr = parts weight per hundred rubber

<sup>B</sup>N-cyclohexyl-2-benzothiazol sulphenamide

<sup>C</sup>N-(1,3-Dimethylbutyl)-N'-phenyl-p-phenylenediamine

Table I: Cure packages and crosslink densities for the three test compounds

Table I: Cure packages and crosslink densities for the three test compounds